Current Trends in Neurology
Vol. 15, 2021

Original Article

The spatial and temporal dynamics of microglia cells in experimental focal cerebral ischemia

Cyrus Wing-Chung Cheng[1] and George Kwok-Chu Wong[2,*]

[1]Faculty of Medicine, The Chinese University of Hong Kong, Hong Kong SAR;
[2]Division of Neurosurgery, Department of Surgery, Prince of Wales Hospital,
The Chinese University of Hong Kong, Hong Kong SAR, China

ABSTRACT

Microglia cells are inflammatory cells of the central nervous system. Following a stroke, cerebral ischemia activates the microglia cells into a diverse range of phenotypes, each with different physical characteristics, surface markers and secretory products, to mediate, augment or suppress the inflammatory process in the brain. We hope to characterize the behavior of these cells to elucidate their role in the inflammatory process. We developed a middle cerebral artery obstruction (MCAO) model on male Sprague-Dawley rats (250-280g) to simulate transient cerebral ischemia by inserting a 4-0 silicone-coated suture through the external carotid artery and the internal carotid artery to occlude the middle carotid artery. After 60 minutes, the filament was removed to allow for reperfusion. Functional assessments were performed pre-surgery, and on days 1, 2, 3, 5, and 7 post-surgery. The animals were subsequently sacrificed. Their brains were double-stained with immunofluorescent Tmem119 and Iba1 antibodies for immunofluorescence analysis. The results were compared to a sham group which received the same surgery bar the insertion of suture. The MCAO model produced consistent neurological deficits in the rats. Immunofluorescence staining showed that the number of microglia cells, the length of microglia cell processes and the surface area occupied by microglia cells fluctuated post- MCAO surgery but did not show any trends. The changes in the physical characteristics of the microglia cells suggest that there is a change of microglia cell phenotypes with time following transient focal cerebral ischemia. We described how future research can better characterize these changes and how RNA profiling and Western Blotting can be used to identify and define the microglia cell phenotypes present following transient focal cerebral ischemia.

KEYWORDS: microglia cells, neuroinflammation, focal cerebral ischemia, ischemic stroke, animal model.

INTRODUCTION

During an ischemic stroke, both cerebral ischemia and cell death induce a series of inflammatory responses in the Central Nervous System (CNS), collectively known as neuro-inflammation [1-3]. Microglia cells have a critical role in neuro-inflammation. They are the major resident immune cells in the CNS and the major trigger of the innate immune response [4, 5]. Microglia cells communicate with astrocytes, neutrophils, dendritic cells, lymphocytes, and pericytes, and participate in the inflammation in the brain parenchyma, the blood brain barrier, and inside the blood vessel [6-17]. Interestingly, the activated microglia cells can be pro-inflammatory and anti-inflammatory. In the pro-inflammatory state, they release pro-inflammatory cytokines, reactive species and proteases to induce inflammation, while in the anti-inflammatory state, they release not only anti-inflammatory mediators,

*Corresponding author
georgewong@surgury.cuhk.edu.hk

but also growth factors and neurotropic factors to reduce inflammation, support neurogenesis and neuroplasticity for recovery [1-3, 17, 18]. Microglia cells also contribute to recovery by acting as phagocytes [18]. Stroke therapies targeting neuro-inflammation show great promise as neuro-inflammation takes days to develop and may persist for months, which translates to a long time window for treatment. Microglia cells can polarize into a spectrum of phenotypes which each have different levels of pro-inflammatory and/or anti-inflammatory activity in response to the microenvironment of the CNS. Therefore, it is valuable to characterize the spatial-temporal dynamics of microglial cell polarization post cerebral ischemia.

MATERIALS AND METHODS

Male, wild-type Sprague Dawley rats, 12 weeks old, 250-280 g were obtained from Laboratory Animal Services Center, Chinese University of Hong Kong. The animals were housed in cages with free access to food and clean water in a room maintained under constant temperature and humidity with 12 h light/dark cycles for one week for acclimatation before the experiments. Before the surgery, we tested their neurological functioning according to the Bederson Scale (Table 1) and the Modified Neurological Severity Scores (mNSS) (Table 2).

The rats were then anesthetized with ketamine (100 mg/kg)/ xylazine (10 mg/kg) intraperitoneally. An electric heating pad was placed under the surgical mat to prevent hypothermia of the animal. The eyes of the rats were covered by an ointment for protection from corneal drying and trauma. A midline neck incision was made. The underneath soft tissues and muscles are retracted to the sides to reveal the common carotid artery, the external carotid artery, and the internal carotid artery [21]. The branches of the external carotid artery (ECA) were cauterized to prevent bleeding. Microvascular clamps were placed at the distal end of the internal carotid artery (ICA) and the distal end of the common carotid artery (CCA) near its bifurcation for temporary blood flow occlusion. A knot was placed at the distal end of the ECA and tightened to prevent the backflow of blood. Two knots were placed at the proximal part of the ECA before the bifurcation and left loose to allow for the insertion

Table 1. The Bederson scale [19].

Degree of Deficit	Description of Deficit	Score
Normal	Both forepaws reach out	0
Mild	Flexion of contralateral limb	1
Moderate	Decreased resistance to lateral push without circling	2
Severe	Decreased resistance to lateral push with circling	3

of the monofilament. A small incision was made distal to the knot with a pair of micro-scissors. Commercially available silicone-rubber coated 4-0 nylon microfilaments (Doccol Corporation, USA) were inserted into the ECA past the two knots. The two knots were tightened to secure the monofilament. The ECA was cauterized distally and manipulated so that the microfilament points towards the ICA. The microvascular clamp placed on the ICA was removed, and the monofilament was advanced into the ICA until slight resistance was felt. The monofilament was manipulated to course medially to avoid the pterygopalatine artery. Around 20 mm of the microfilament was inserted past the CCA bifurcation. The monofilament was withdrawn after 60 minutes. The ECA was cauterized to prevent bleeding. The microvascular clamp placed at the CCA was then removed. After confirming the restoration of anterograde blood flow into the ICA, and no surgical site bleeding, all knots and surgical instruments were removed. The midline neck incision was repaired using surgical suture. 1.0 ml of phosphate buffered saline (PBS) was given intraperitoneally for volume replenishment. Buprenorphine was also given immediately and twice daily for 3 days for analgesia. For the sham surgery, the same procedure barring the insertion of microfilament was done on separate rats.

Post surgery, the animals were allowed to recover for 1/ 2/ 3/ 5/ 7 days. We tested their neurological functioning again before they were sacrificed. Following transcardiac perfusion with PBS, the animals were decapitated to obtain the brain. We examined the skull base for blood, which would suggest subarachnoid hemorrhage (SAH). Animals with SAH were excluded. The brain was sectioned into 2 mm slices using a coronal brain matrix starting from the caudal end of the brain. The first brain

Table 2. The modified neurological severity scores [20].

Motor Tests (a + b)	Maximum: 6
a. Raising rat by tail	Maximum: 3
•Flexion of forelimb	1
•Flexion of hindlimb	1
•Head moved > 10° to vertical axis within 30s	1
b. Placing rat on floor	Maximum: 3
•Normal Walk	0
•Inability to walk straight	1
•Circling toward the paretic side	2
•Falls to the paretic side	3
Sensory Tests	Maximum: 2
•Placing test (Visual and Tactile test)	1
•Proprioceptive test (Deep sensation, Pushing paw against table edge to stimulate limb muscles)	1
Beam balance tests	Maximum: 6
Balances with steady posture	0
Grasps the side of beam	1
Hugs the beam, One limb falls off the beam	2
Hugs the beam, Two limb falls off the beam; or spins on the beam (>60s)	3
Attempts to balance on the beam but falls off (>40s)	4
Attempts to balance on the beam but falls off (>20s)	5
Falls off the beam; or no attempt to balance on the beam (<20s)	6
Reflex absence and abnormal movements	Maximum: 4
Pinna reflex (head shake when auditory meatus is touched)	1
Corneal reflex (eye blink) when cornea is lightly touched with cotton)	1
Startle reflex (motor response to a brief noise from snapping a clipboard paper)	1
Seizures, myoclonus, myodystonia	1
Maximum points	**Total: 18**

section was placed in 1% 2,3,5-triphenyltetrazolium chloride (TTC) (Sigma Aldrich) at 4 °C overnight for infarct verification. The second and the following brain sections were transferred to 4% paraformaldehyde (PFA) at room temperature for 48 h for fixation. They were then sent for paraffin embedding, after which they were trimmed into 5 µm thick sections with a microtome and transferred to glass slides for immunofluorescence staining. The brain slides were deparaffinized with xylene and ethanol, and incubated in 0.3% hydrogen peroxide (H_2O_2) for 10 minutes to quench the activity of endogenous peroxidase. They were then treated with 0.1% Triton X-100 buffered in 0.1% sodium citrate solution at 100 °C for 20 minutes for antigen retrieval. 10% normal goat serum blocking buffer was added to the slides and left for incubation for 2 hours at room temperature to prevent non-specific binding of antibodies to the sample. Primary antibodies Rabbit monoclonal Anti-Iba1 (1:200; Abcam, #ab178846) and Mouse monoclonal Anti-Tmem119 (1:200; Synaptic Systems, #400211), diluted in 10% normal goat serum, were added to the slides and left for incubation overnight at 4 °C. The secondary antibodies Donkey Anti-mouse IgG (Alexa Fluor® 488) (1:200; Abcam, #ab150109)

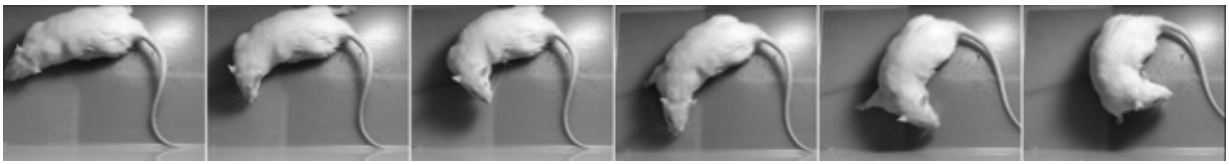

Figure 1. All the rats showed ipsilateral hemiparesis 1 day after MCAO surgery.

and Donkey Anti-rabbit IgG (Alexa Fluor® 594) (1:200; Abcam, #ab150076) were added to the brain sections and left for incubation at room temperature for 2 hours. The brain slides were mounted with 4′,6-diamidino-2-phenylindole (DAPI) (Abcam, #ab104139). Immunofluorescent images were acquired with the Nikon Eclipse-Ti inverted microscope. Quantification of microglia cells and the measurement of the number of microglia cell processes, the length of microglia cell processes and the area of microglia cells were performed with Image J.

RESULTS AND DISCUSSION

General observations and functional assessments of the MCAO model

40 rats were used in the study. 35 rats received the MCAO surgery and 5 rats received the sham surgery. The mortality rate of the MCAO surgery and the sham surgery were 5/35= ~14.2% and 0%, respectively. All rats became active again within the first 1.5 h post surgery. They were weak, low in energy and disoriented. They were tremulous as they attempted to return to the prone position. The rats that received the MCAO surgery also had ipsilateral ptosis and hemiparesis (Figures 1, 2). The rats that received the sham surgery did not display these deficits.

The Bederson Scale rates the animal as normal (0), or with mild deficit (1), moderate deficit (2), or severe deficit (3). All rats scored 0 before the surgeries. The rats that received the MCAO surgery and were sacrificed on D1, D2, D3, D5 and D7 scored 3, 3, 3, 2, and 2, respectively (Figure 3). The rats that received the sham surgery scored 0 before they were sacrificed. The neurological deficits suggested a high likelihood that a stroke had been induced. They also showed that motor function improved with time. For the Modified Neurological Severity Scores, a higher score reflects more severe neurological deficits. All rats scored 0 before the surgeries. The rats that received the sham surgery scored 0 before they were sacrificed. The rats that received the MCAO surgery and were sacrificed on D1, D2, D3, D5 and D7 scored 17, 14, 12, 7, and 4, respectively (Figure 4). This again showed that neurological functioning improved with time. The sub-scores suggested that the different domains of neurological functioning improved at different rates.

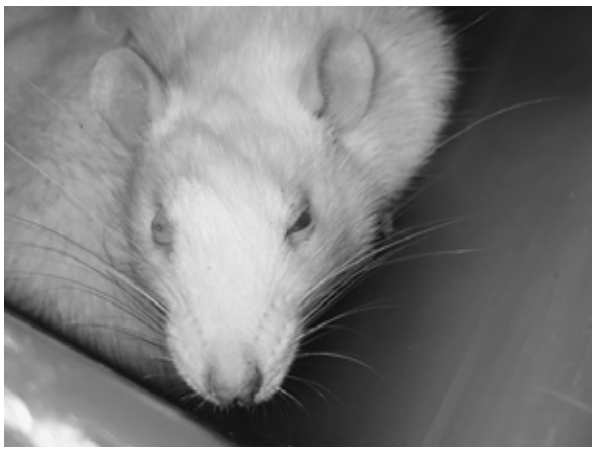

Figure 2. All rats had ipsilateral ptosis after MCAO surgery.

Post-mortem confirmation of MCAO model

In viable tissues, dehydrogenase enzymes reduce TTC into the red-staining formazan; thus the tissue becomes red in color [22]. Infarcted tissues have no dehydrogenase activity and thus remain pale. The staining with TTC showed that all rats that received the MCAO surgery had observable infarcts. The rats that were sacrificed on D1 had an infarct covering more than 50% of the ipsilateral brain that extends from the cortex into the hippocampus and the striatum. The infarcts in those that were sacrificed on later days shrunk in size and receded laterally (Figure 5). This suggested a continuous repair process was present in the CNS.

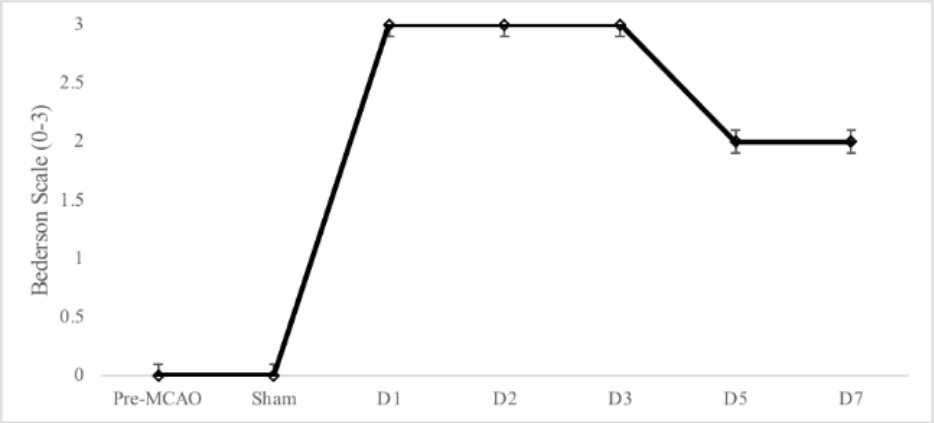

Figure 3. The Bederson Scale.

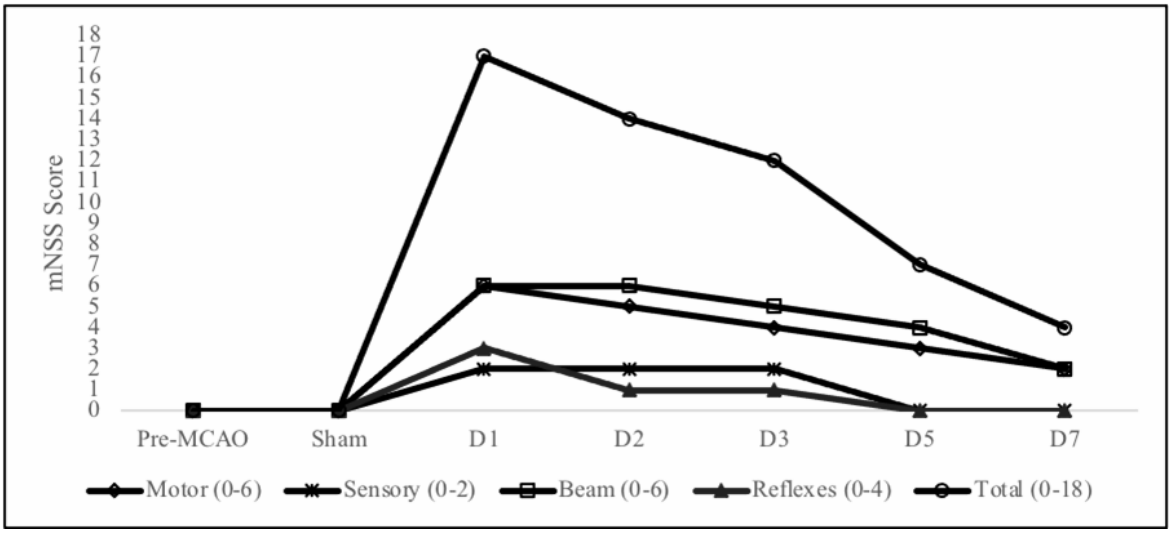

Figure 4. The Modified Neurological Severity Scores (mNSS).

The brain sections were stained with Ionized calcium binding adaptor molecule (Iba1) and Transmembrane protein 119 (Tmem119) immunofluorescent staining. Anti-Iba1 antibodies provide good resolution of microglia cells for the study of their morphology. However, Iba1 is also expressed on macrophages. To label microglia cells, the microglia cell-specific Tmem119 is also used.

Microglia cells were present throughout the cortex and the striatum. There were no statistically significant differences in the number of microglia cells in the ipsilateral side and the contralateral side, and the cortex and the hippocampus. On the contralateral side, the number increased from D1 to D3, and decreased afterwards. On the ipsilateral side, the number fluctuated with time and did not form a trend. More data is needed to ascertain its statistical significance.

The total and average number of microglia processes were lower on the ipsilateral side than the contralateral side. These observations probably reflect more microglia cell activation on the ipsilateral side, as the 'amoeboid' form typical of activated microglia cells has less and shorter processes. The average number of microglia processes across the cortex and hippocampus had similar standard deviations of between 1.5 and 2.0. This suggests that microglia cell populations consist of cells

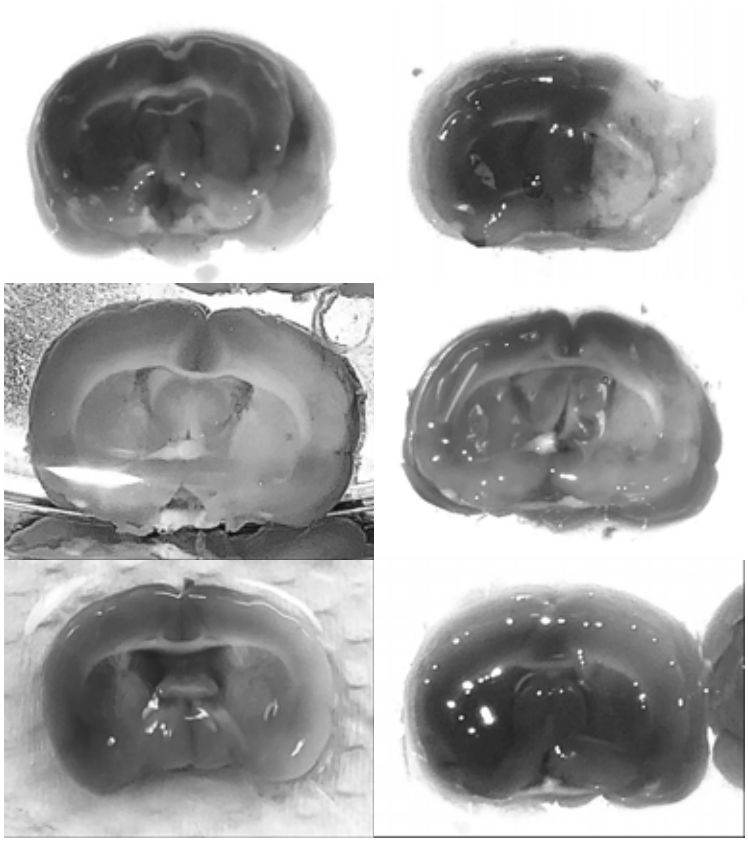

Figure 5. Brain sections after treatment with TTC. Top Left: Sham; Top Right: D1; Middle Left: D2; Middle Right: D3; Lower Left: D5; Lower Right: D7.

with different znumber of processes across different regions in different time points, potentially due to the need for these cells to perform diverse functions. The trend of smaller variations in the average number of microglia processes seen on the ipsilateral side than the contralateral side is also compatible with this postulation, as more microglia cells on this side may be activated as they are closer to where the ischemia occurred. The total and average lengths of microglia processes were lower on the ipsilateral side than the contralateral side. The average lengths of microglia processes had similar standard deviations of around 30 μm. These observations align with the hypothesis we suggested above. The total and average surface area occupied by microglia cells were smaller on the ipsilateral side than on the contralateral side. When microglia cells are activated, they become globular in shape to perform phagocytosis; thus the cell body should increase in size. Accordingly, the surface area occupied by microglia cells is expected to increase. However, this was not seen. One possible reason is that the reduction of surface area caused by the shortening and reduction of microglia processes was nullified by the increase caused by the change of microglia cell shape. The standard deviation of average surface area was smaller on the ipsilateral side than the contralateral side. The observation that microglia cells have more uniform surface area on the ipsilateral side aligns with the hypothesis we suggested above.

Morphological analysis has been central to microglia cell research. It was suggested that microglia cells shift between a resting state, when they become ramified, and an active state, when they become amoeboid in shape, according to environmental signals to perform different functions [17, 23-25]. It was thought that certain molecules are inductive of this change, and thus researchers had been eager to identify them in hope to modulate the microglia cells. Microglia cell morphology was used as litmus test to facilitate the research of these two states.

However, we showed that the changes in the length of microglia cell processes and surface area occupied by microglia cells post-MCAO surgery fluctuated but did not show any trends. Interestingly, one study also reported patterns of change of microglia cells following cerebral ischemia that differed from what the classical microglia cell transition theory suggests. In that study, the microglia cells first retracted their processes at 3-12 h post-MCAO surgery, then extended their processes from 24 h onwards [26]. This suggested that the morphological change of microglia cells post-cerebral ischemia is non-linear. Accordingly, future studies should take more time points to characterize the change in time more precisely. Furthermore, more sophisticated metrics should be used to characterize microglia cell morphology. For the analysis of microglia cell processes, microglia cells may be skeletonized, whereby the computer program uses straight lines to construct a representation of the shape of the cell [27-31]. Information including the length of microglia cell processes and the number of microglia cell processes can be inferred from the length of the straight lines, and the number of endpoints and junctions of these straight lines present [27-31]. Fractal analysis may be used to quantify the complexity, the density and span ratio of the microglia cells present [32]. It measures the complexity of the contour of each microglia cell using the endpoints and the lengths of its processes [32]. It uses geometric functions to derive the density and the span ratio of microglia cells, which reflect the size and the shape of microglia cells, respectively.

On the other hand, more recent research suggests that microglia cells exist in more states than the two named, and that microglia morphology is not a reliable marker of microglia cell state [33-35]. Thus, microglia cell activation should be studied by alternative ways. It was reported that microglia cells within the same anatomical region display different morphological characteristics if they are distributed inside and outside the infarct core differently. One study described that microglia cells in one cortical region displayed three types of morphology because they received different amounts of blood flow [26, 36]. Microglia cells in regions that received normal blood flow were in the resting state characterized by ramified processes, while those in the infarct core and the surrounding area were in the activated state characterized by hypertrophic, amoeboid shaped cell bodies [26, 36]. A third group of cells that were sandwiched between these two groups of cells had short and stout processes [26, 36]. Another study described a similar picture, in which amoeboid shaped, activated microglia cells were present inside the infarct core, while highly ramified, resting microglia cells were present right outside the infarct core [37]. This study attributed the morphological differences between the two groups of microglia cells to the astrocytic scar in between them [37]. It suggested that those inside the infarct core were in the activated state to perform phagocytosis. As they could be harmful to the other brain regions that did not have an infarct, they were sealed off by the astrocytic scar which serves to protect the rest of the brain [37]. Although a common picture of microglia cell morphology after cerebral ischemia have been described, the lack of consensus on what caused their morphology to change warrants further investigation. As microglia cells perform their actions by either expressing receptors on their cellular surface or secreting signaling molecules, the expression levels of the related genes, and the amount of protein products produced can be used to define the microglia cell's phenotype [4, 5]. Should the expression level of genes and/or the amount of protein products produced correlate with microglia cell function, the corresponding molecular pathway and targets will also be revealed.

CONCLUSION

Ischemic stroke presents a heavy disease burden globally and novel therapeutics that improve post-stroke outcome are needed. In our study, we developed and functionally verified an animal model that could produce infarct and model focal cerebral ischemia. We confirmed the observation that microglia cells exhibit diverse cell morphology after focal cerebral ischemia. We also found out that the physical characteristics fluctuated post-MCAO surgery but did not show any trends. The changes in the physical characteristics of the microglia cells suggest that there is a change of microglia cell phenotypes with time following transient focal cerebral ischemia. We described how future research can better characterize these changes. In addendum, RNA profiling and Western

Blotting can be used to identify and define the microglia cell phenotypes present following transient focal cerebral ischemia.

ACKNOWLEDGEMENTS

N/A.

CONFLICT OF INTEREST STATEMENT

N/A.

REFERENCES

1. Iadecola, C. and Alexander, M. 2001, Current opinion in neurology, 14(1), 89-94.
2. Huang, J., Upadhyay, U. M. and Tamargo, R. J. 2006, Surgical neurology, 66(3), 232-45.
3. Brea, D., Sobrino, T., Ramos-Cabrer, P. and Castillo, J. 2009, Cerebrovascular diseases, 27(Suppl. 1), 48-64.
4. Kettenmann, H., Hanisch, U. K., Noda, M. and Verkhratsky, A. 2011, Physiological reviews, 91(2), 461-553.
5. Norris, G. T. and Kipnis, J. 2019, Journal of Experimental Medicine, 216(1), 60-70.
6. Liddelow, S. A., Guttenplan, K. A., Clarke, L. E., Bennett, F. C., Bohlen, C. J., Schirmer, L., Bennett, M. L., Münch, A. E., Chung, W. S., Peterson, T. C. and Wilton, D. K. 2017, Nature, 541(7638), 481-7.
7. Otxoa-de-Amezaga, A., Miró-Mur, F., Pedragosa, J., Gallizioli, M., Justicia, C., Gaja-Capdevila, N., Ruíz-Jaen, F., Salas-Perdomo, A., Bosch, A., Calvo, M. and Márquez-Kisinousky, L. 2019, Acta neuropathologica, 137(2), 321-41.
8. Neumann, J., Sauerzweig, S., Rönicke, R., Gunzer, F., Dinkel, K., Ullrich, O., Gunzer, M. and Reymann, K. G. 2008, Journal of Neuroscience, 28(23), 5965-75.
9. Fischer, H. G. and Reichmann, G. 2001, The Journal of Immunology, 166(4), 2717-26.
10. Almolda, B., Gonzalez, B. and Castellano, B. 2011, Front Biosci., 16(1), 1157-71.
11. Magnus, T., Chan, A., Linker, R. A., Toyka, K. V. and Gold, R. 2002, Journal of Neuropathology & Experimental Neurology, 61(9), 760-6.
12. Guillemin, G. J. and Brew, B. J. 2004, Journal of leukocyte biology, 75(3), 388-97.
13. Berchtold, D., Priller, J., Meisel, C. and Meisel, A. 2020, Brain Pathology, 30(6), 1208-18.
14. Crack, P. J. and Wong, C. H. 2008, Current medicinal chemistry, 15(1), 1-4.
15. del Zoppo, G. J. 2009, Neuroscience, 158(3), 972-82.
16. Chen, A. Q., Fang, Z., Chen, X. L., Yang, S., Zhou, Y. F., Mao, L., Xia, Y. P., Jin, H. J., Li, Y. N., You, M. F. and Wang, X. X. 2019, Cell death & disease, 10(7), 1-8.
17. Patel, A. R., Ritzel, R., McCullough, L. D. and Liu, F. 2013, International journal of physiology, pathophysiology and pharmacology, 5(2), 73.
18. Fu, R., Shen, Q., Xu, P., Luo, J. J. and Tang, Y. 2014, Molecular neurobiology, 49(3), 1422-34.
19. Modo, M. 2009, Journal of Experimental Stroke & Translational Medicine, 2009, 02(02), 52-68.
20. Guo, X-bin., Deng, X. and Wei, Y. 2017, Scientific Reports, 7(1), 4164.
21. Savastano, L. E., Castro, A. E., Fitt, M. R., Rath, M. F., Romeo, H. E. and Muñoz, E. M. 2010, Journal of Neuroscience Methods, 192(1), 22-33.
22. Liu, F., Schafer, D. P. and McCullough, L. D. 2009, Journal of neuroscience methods, 179(1), 1-8.
23. Streit, W. J., Mrak, R. E. and Griffin, W. S. 2004, Journal of neuroinflammation, 1(1), 1-4.
24. Lynch, M A. 2009, Molecular neurobiology, 40(2), 139-56.
25. Zhang, S. 2019, Stroke and vascular neurology, 4(2), 71-74.
26. Buscemi, L., Price, M., Bezzi, P. and Hirt, L. 2019, Scientific Reports, 9(1), 507.
27. Karperien, A., Ahammer, H. and Jelinek, H. F. 2013, Frontiers in Cellular Neuroscience, 7, 3.
28. Morrison, H., Young, K., Qureshi, M., Rowe, R. K. and Lifshitz, J. 2017, Scientific Reports, 7(1), 13211.
29. Young, K. and Morrison, H. 2018, Journal of Visualized Experiments, 136, 57648.
30. Fernández-Arjona Mdel, Grondona, J. M., Granados-Durán, P., Fernández-Llebrez, P. and López-Ávalos, M. D. 2017, Frontiers in Cellular Neuroscience, 11, 235.

31. Heindl, S., Gesierich, B., Benakis, C., Llovera, G., Duering, M. and Liesz, A. 2018, Frontiers in Cellular Neuroscience, 12, 106.
32. York, E. M., LeDue, J. M., Bernier, L-P. and MacVicar, B. A. 2018, Eneuro, 5(6), ENEURO.0266-18.2018.
33. Bell-Temin, H., Culver-Cochran, A., Chaput, D., Carlson, C., Kuehl, M., Burkhardt, B., Bickford, P., Liu, B. and Stevens, S. 2015, Molecular & Cellular Proteomics, 14(12), 3173-84.
34. Miron, V. E., Boyd, A., Zhao, J. W., Yuen, T. J., Ruckh, J. M., Shadrach, J. L., van Wijngaarden, P., Wagers, A. J., Williams, A. and Franklin, R. J. 2013, Nature neuroscience, 16(9), 1211-8.
35. Zhang, L., Zhang, J. and You, Z. 2018, Frontiers in cellular neuroscience, 12, 306.
36. Li, L., Lundkvist, A., Andersson, D., Wilhelmsson, U., Nagai, N. and Pardo, A. C. 2007, Journal of Cerebral Blood Flow & Metabolism, 28(3), 468-81.
37. Weinstein, J. R., Koerner, I. P. and Möller T. 2010, Future Neurol., 5(2), 227-246.